

Robust adaptive MPC using control contraction metrics

András Sasfi¹, Melanie N. Zeilinger², Johannes Köhler²

¹*Automatic Control Laboratory, ETH Zürich, Zürich CH-8092, Switzerland*

²*Institute for Dynamic Systems and Control, ETH Zürich, Zürich CH-8092, Switzerland*

Abstract

We present a robust adaptive model predictive control (MPC) framework for nonlinear continuous-time systems with bounded parametric uncertainty and additive disturbance. We utilize general control contraction metrics (CCMs) to parameterize a homothetic tube around a nominal prediction that contains all uncertain trajectories. Furthermore, we incorporate model adaptation using set-membership estimation. As a result, the proposed MPC formulation is applicable to a large class of nonlinear systems, reduces conservatism during online operation, and guarantees robust constraint satisfaction and convergence to a neighborhood of the desired setpoint. One of the main technical contributions is the derivation of corresponding tube dynamics based on CCMs that account for the state and input dependent nature of the model mismatch. Furthermore, we online optimize over the nominal parameter, which enables general set-membership updates for the parametric uncertainty in the MPC. Benefits of the proposed homothetic tube MPC and online adaptation are demonstrated using a numerical example involving a planar quadrotor.

Key words: model predictive control; tube MPC; control contraction metrics; nonlinear systems; control of constrained systems; uncertain systems;

1 Introduction

Some of the most challenging control problems are characterized by nonlinear uncertain dynamics and safety critical constraints. Optimization-based control techniques, such as model predictive control (MPC) [40], can offer high performance control for nonlinear systems, while respecting general state and input constraints. However, the desired closed-loop properties (stability, performance, constraint satisfaction) are in general not preserved under model uncertainty. In this paper, we develop a robust adaptive MPC framework that robustly ensures such closed-loop properties for a large class of uncertain nonlinear systems, while incorporating online model updates to reduce conservatism. This is achieved by introducing a novel *robust* MPC design, including a general method to incorporate *adaptive* model updates.

Robust MPC methods for nonlinear uncertain systems

Robust MPC (RMPC) methods typically ensure constraint satisfaction despite model uncertainty by predicting a tube/funnel over the prediction horizon that contains all uncertain trajectories. There exists a wide range of nonlinear RMPC approaches in the literature [14, 22, 31, 45, 50], which vary strongly in their conser-

vatism or computational complexity. For example, System Level Synthesis [22] allows to jointly optimize over a linear feedback and optimization over cross sections of the tube results in great flexibility [14, 45, 50]. However, these methods can result in a drastic increase of the computational complexity that may impede real-time implementation. The trade-off between complexity and conservatism is well-understood in case of linear systems (cf., e.g., [4, 21]). In this work, we focus on the design of nonlinear robust MPC methods with small computational complexity, ideally close to nominal MPC. In case of linear systems, the tube-based RMPC schemes in [34, 35, 38] achieve this by performing more expensive computations related to reachability analysis and invariant sets offline. This results in a parameterized tube, e.g., in the form of a polytope or ellipsoid, which is simple to predict over the prediction horizon. Therein, computational efficiency is ensured by performing more expensive computations related to reachability analysis and invariant sets offline, resulting in a parameterized tube, e.g., in the form of a polytope or ellipsoid, that is simple to predict over the prediction horizon. Correspondingly, utilizing similar concepts for nonlinear systems requires an offline computation of (parameterized) robust positive invariant sets, which can be done using simple ellipsoidal sets [46, 49], general incremental Lyapunov functions [3, 20], and more recently con-

trol contraction metrics (CCMs) [42, 43, 51]. These invariant sets can then be used as a *rigid* tube around a nominal prediction to obtain a simple nonlinear RMPC scheme [3, 42, 43, 46, 49, 51], compare also [34]. However, such a rigid tube is conservative if the model mismatch depends on the state or input, e.g., due to parametric uncertainty. Such effects can be better captured using a *homothetic* tube [17, 19, 20, 26, 39], i.e., the tube scaling depends on the nominal trajectory, compare also [28, 38]. In this paper, we extend and unify these concepts by deriving a homothetic tube MPC framework for nonlinear uncertain systems based on general CCMs.

Parameter updates in robust adaptive MPC

Model mismatch is often partially due to inaccurate system knowledge and performance may be enhanced by incorporating online model updates in RMPC frameworks [13]. In case of linearly parameterized models with bounded disturbance, we can efficiently update parameter sets using set-membership estimation [17, 28] or Lyapunov-type arguments [1, 12]. Especially, utilizing set-membership estimation in RMPC schemes to reduce uncertainty is well-established for linear systems [28–30, 36, 44]. However, since most (nonlinear) RMPC frameworks explicitly depend on a nominal trajectory with some nominal parameter, most resulting RAMPC schemes (cf. [1, 8, 12, 16, 17, 26]) require restrictive additional assumptions to ensure recursive feasibility under model updates, such as the restriction of the parameter set to balls/hypercubes instead of general ellipsoids/polytopes. In this paper, we show how to incorporate general parameter updates in nonlinear RMPC schemes without posing such additional restrictions, resulting in a flexible RAMPC scheme.

Contribution

The theoretical contribution of this work is twofold. First, we propose a novel robust MPC framework for nonlinear continuous-time systems by deriving a homothetic tube propagation for general CCMs. Second, we present a method that allows us to naturally incorporate online model updates, resulting in a RAMPC framework.

To formulate the proposed RMPC scheme, we first extend existing results on (robust) CCMs (cf. [25, 33, 43, 48, 51]) by deriving a differential equation for the tube scaling, resulting in a homothetic tube that contains all possible nonlinear uncertain trajectories. In particular, the derived tube dynamics directly use state and input dependent bounds on the model mismatch, thus avoiding the conservatism of constant bounds [43, 51]. To the best knowledge of the authors, this is also the first result on tube MPC schemes that rigorously shows that the CCM conditions are only needed on the constraint set, without imposing additional assumptions.

Compared to existing homothetic tube MPC formulations (cf. [19, 20, 26, 39]), the reliance on established CCM synthesis tools (cf. [33, 43, 51]) ensures the practical applicability to a large class of uncertain nonlinear systems.

We incorporate online model updates by using set-membership estimation for the parametric uncertainty. In contrast to existing approaches, we propose to additionally optimize over the nominal parameter that characterizes the nominal trajectory. This seemingly trivial modification retains the desired flexibility of the model updates without requiring the additional restrictions needed in related work [1, 8, 12, 16, 17, 26]. As a result, the derived RAMPC scheme can also directly track steady-states which explicitly depend on the unknown parameter.

Overall, the resulting homothetic tube RAMPC framework guarantees recursive feasibility, constraint satisfaction, and convergence to a neighborhood of the desired steady-state. We demonstrate the benefits of the homothetic tube MPC and online model updates using the planar quadrotor example from [51].

Outline

Section 2 introduces the problem setup and outlines the general RAMPC approach. Section 3 presents the main results, including the novel homothetic tube propagation based on CCMs, the proposed RAMPC scheme, and the theoretical analysis. Finally, Section 4 presents a numerical example and Section 5 provides a conclusion.

Notation

The set of non-negative real numbers is $\mathbb{R}_{\geq 0}$, while $\mathbb{I}_{[a,b]}$ is the set of integers in the interval $[a, b]$. The i -th element of a vector x is denoted by $[x]_i$. Furthermore, $[X]_{:,k}$ is the k -th column of X . The zero matrix and the identity matrix of appropriate dimensions are denoted by 0 and I , respectively. We use the notation $\langle A \rangle = A + A^\top$ for square matrices $A \in \mathbb{R}^{n \times n}$. The set of positive definite matrices of size $n \times n$ is \mathbb{S}_n^+ , and $A \preceq B$ indicates that $B - A$ is positive semi-definite. The quadratic norm of a vector x w.r.t. a positive definite matrix M is denoted by $\|x\|_M := \sqrt{x^\top M x}$. The Cholesky decomposition of a positive definite matrix is denoted by $\left(M^{\frac{1}{2}}\right)^\top M^{\frac{1}{2}} = M$, yielding $\|x\|_M = \left\|M^{\frac{1}{2}}x\right\|$. Throughout the paper, we indicate the time dependence by $x(t)$ for actual trajectories or $z_{t|t_k}$ for predicted trajectories at time t_k . For a continuously differentiable function $f : \mathbb{R}^a \times \mathbb{R}^b \rightarrow \mathbb{R}^c$, $f(x, u)$, the partial and total derivative w.r.t. x evaluated at some point $(x, u) = (z, v)$ is defined as $\left.\frac{\partial f}{\partial x}\right|_{(z,v)} \in \mathbb{R}^{c \times a}$ and

$\left. \frac{df}{dx} \right|_{(z,v)}$, respectively. Similarly, we abbreviate the total time derivative by $\dot{f}(x, u) := \left. \frac{df}{dt} \right|_{(x,u)}$.

2 Preliminaries

We first present the considered problem setup (Sec. 2.1). Then, we outline how the problem is addressed using the proposed homothetic tube RAMPC scheme (Sec. 2.2).

2.1 Problem setup

We consider a continuous-time nonlinear system

$$\dot{x}(t) = f_w(x(t), u(t), \theta, d(t)), \quad x(0) = x_0, \quad t \geq 0, \quad (1)$$

with state $x(t) \in \mathbb{R}^n$, initial state $x_0 \in \mathbb{R}^n$, input $u(t) \in \mathbb{R}^m$, disturbance $d(t) \in \mathbb{R}^q$, and constant model parameter $\theta \in \mathbb{R}^p$. The disturbance $d(t)$ and the model parameter θ are unknown and satisfy a known bound $d(t) \in \mathbb{D}$, $t \geq 0$, $\theta \in \Theta_0$ with polytopes $\Theta_0 \subseteq \mathbb{R}^p$, $\mathbb{D} \subseteq \mathbb{R}^q$ and $0 \in \mathbb{D}$, and the state $x(t)$, $t \geq 0$ can be measured. Furthermore, we assume that the dynamics f_w are affine in u , d , θ , i.e., we have

$$f_w(x, u, \theta, d) = f(x) + B(x)u + G(x, u)\theta + E(x)d,$$

with G affine in u , i.e., f_w is affine in u , d and θ , respectively. Throughout the paper, we assume that f_w is continuously differentiable and Lipschitz continuous and $u(t)$ and $d(t)$ are piecewise continuous, which implies existence of a unique solution $x(\cdot)$ to the system (1), see [15, Thm. 3.2].¹ The system is subject to state and input constraints

$$(x(t), u(t)) \in \mathbb{Z}, \quad t \geq 0, \quad (2)$$

where \mathbb{Z} is a compact set defined by

$$\mathbb{Z} := \{(x, u) \in \mathbb{R}^{n+m} \mid h_j(x, u) \leq 0, j \in \mathbb{I}_{[1,r]}\}. \quad (3)$$

We denote the projection of \mathbb{Z} on x by \mathbb{Z}_x .

The overall goal can be summarized in the following conceptual infinite-horizon optimal control problem:

$$\begin{aligned} & \min_{\pi(\cdot)} \max_{d(\cdot) \in \mathbb{D}, \theta \in \Theta_0} \mathcal{J}_\infty(x(0), \pi(\cdot), d(\cdot), \theta) \\ \text{s.t.} \quad & u(t) = \pi(x(\cdot), t), \\ & (x(t), u(t)) \in \mathbb{Z}, \\ & \dot{x}(t) = f_w(x(t), u(t), \theta, d(t)), \quad t \geq 0. \end{aligned} \quad (4)$$

¹ Similarly to (12a)–(12b), one can show that the feedback $\kappa(x, z, v)$ in Proposition 2 is Lipschitz continuous w.r.t. x . Hence, existence and uniqueness of the solution to (1) remain valid under the feedback κ .

The goal is to find a causal policy π , that minimizes some cost \mathcal{J}_∞ under the worst-case disturbance and parameter, while robustly satisfying the state and input constraints.

2.2 General RAMPC approach

Problem (4) is intractable in this form due to the optimization over a general policy π that depends on all past data and the difficulty to compute the exact (disturbance) reachable set for nonlinear systems. In the following, we provide a high-level description of how we compute a feasible solution to Problem (4) by using a finitely parametrized policy π and an over-approximation of the possible state trajectories $x(t) \in \mathbb{T}_t$, where \mathbb{T}_t is called a tube. As common in tube-based robust MPC formulations, this is achieved by defining a nominal state and input trajectory z_t, v_t based on some nominal parameter $\bar{\theta} \in \Theta_0$ with the nominal dynamics $\dot{z}_t = \bar{f}(z_t, v_t, \bar{\theta}) := f_w(z_t, v_t, \bar{\theta}, 0)$. The policy is then given as a feedback law $\kappa : \mathbb{R}^n \times \mathbb{Z} \rightarrow \mathbb{R}^m$ parametrized by the nominal trajectories, i.e., $\pi(x(\cdot), t) = \kappa(x(t), z_t, v_t)$. Furthermore, the tube is parametrized as

$$\mathbb{T}_t = \{x \in \mathbb{R}^n \mid V_\delta(x, z_t) \leq \delta_t\}, \quad t \geq 0, \quad (5)$$

where $V_\delta : \mathbb{R}^n \times \mathbb{R}^n \rightarrow \mathbb{R}_{\geq 0}$ is a later specified Lyapunov-type function and $\delta_t \geq 0$ is a suitable scaling. Given this parametrization, we can provide a feasible solution to Problem (4) with

$$\dot{z}_t = \bar{f}(z_t, v_t, \bar{\theta}), \quad \dot{\delta}_t = f_\delta(z_t, v_t, \delta_t, \bar{\theta}, \Theta_0), \quad (6a)$$

$$(x(t), \kappa(x(t), z_t, v_t)) \in \mathbb{Z}, \quad \forall x(t) \in \mathbb{T}_t, \quad t \geq 0, \quad (6b)$$

where f_δ corresponds to a later derived dynamics for the tube scaling (cf. Sec. 3.2) ensuring $x(t) \in \mathbb{T}_t$, $t \geq 0$. Since the parametrization (5) contains a (not necessarily linear) translation z_t and a scaling δ_t , we refer to it as a homothetic tube MPC due to its similarity to existing approaches for linear systems [28, 38]. In particular, in case V_δ is a polytopic or quadratic function of the error $x - z_t$, we recover the homothetic tube parametrization in [8, 16, 28, 35, 38, 39]. As one of the main technical contributions, in Sections 3.1–3.2 we show how suitable functions κ , V_δ can be constructed offline using CCMS and derive dynamics for the tube scaling δ_t .

For simplicity, we assume that the cost \mathcal{J}_∞ in (4) corresponds to a quadratic tracking stage cost of the form

$$\ell(z, v, \bar{\theta}) = \|z - z_{\text{ref}}(\bar{\theta})\|_Q^2 + \|v - v_{\text{ref}}(\bar{\theta})\|_R^2, \quad (7)$$

with positive definite matrices $Q \in \mathbb{R}^{n \times n}$, $R \in \mathbb{R}^{m \times m}$ and a feasible steady-state and input $(z_{\text{ref}}(\bar{\theta}), v_{\text{ref}}(\bar{\theta})) \in \mathbb{Z}$, $\bar{f}(z_{\text{ref}}(\bar{\theta}), v_{\text{ref}}(\bar{\theta}), \bar{\theta}) = 0$, $\bar{\theta} \in \Theta_0$, which may depend (continuously) on the nominal parameter $\bar{\theta}$ (cf.

also Sec. 3.6). To approximate the infinite-horizon problem (4), we repeatedly solve a finite-horizon problem at every sampling time $t_k = kT_s$, $k \in \mathbb{I}_{\geq 0}$ with sampling period $T_s > 0$, using the standard receding horizon principle from MPC [40]. We incorporate model adaptation by updating the set Θ_0 online at every sampling time t_k using set-membership estimation.

3 Robust adaptive MPC framework

This section derives the proposed RAMPC framework, which is the main result of the paper. First, we use CCMs to construct the homothetic tube (Sec. 3.1–3.2). Next, we present how the initial parameter set Θ_0 can be updated using set-membership estimation (Sec. 3.3), followed by the design of the terminal ingredients (Sec. 3.4). Then, the overall algorithm, including the MPC problem, is described and the theoretical properties are derived (Sec. 3.5). Finally, we provide some discussion, including a qualitative comparison to existing approaches (Sec. 3.6).

3.1 Control contraction metrics

In the following, we show that CCMs provide a natural way to derive the ingredients needed in the homothetic tube design ($V_\delta, \kappa, f_\delta$). In particular, CCMs use the Jacobian of the dynamics f_w to synthesize controllers ensuring (incremental) stability for the nonlinear dynamics [33, 42, 43, 48, 51].

Assumption 1 *There exists a smooth function $M : \mathbb{R}^n \rightarrow \mathbb{S}_n^+$, a continuous function $K : \mathbb{R}^n \rightarrow \mathbb{R}^{m \times n}$, a contraction rate $\rho_c > 0$, and matrices $\underline{M}, \overline{M} \in \mathbb{S}_n^+$, such that for all $(x, u) \in \mathbb{Z}$, and all $\theta \in \Theta_0$, $d \in \mathbb{D}$, the following properties hold:*

$$\dot{M}(x) + \langle M(x)A_{\text{cl}}(x, u, \theta, d) \rangle \preceq -2\rho_c M(x), \quad (8a)$$

$$\underline{M} \preceq M(x) \preceq \overline{M}, \quad (8b)$$

with $\dot{x} = f_w(x, u, \theta, d)$, and

$$A_{\text{cl}}(x, u, \theta, d) := \frac{\partial f_w}{\partial x} \Big|_{(x, u, \theta, d)} + \frac{\partial f_w}{\partial u} \Big|_{(x, u, \theta, d)} K(x).$$

Conditions (8a)–(8b) imply stability of the linearized dynamics with the differential feedback K using the contraction metric M . By integrating this differential form we can obtain stability properties for the nonlinear system. To this end, we denote the set of piece-wise smooth curves $\gamma : [0, 1] \rightarrow \mathbb{R}^n$ with $\gamma(0) = z$ and $\gamma(1) = x$ by $\Gamma(z, x)$, and define $\gamma_s(s) := \frac{\partial \gamma}{\partial s} \Big|_s$. Given a CCM satisfy-

ing Assumption 1, we define a corresponding incremental Lyapunov function V_δ (cf. [33]) as follows:

$$V_\delta(x, z) := \min_{\gamma \in \Gamma(z, x)} \int_0^1 \|\gamma_s(s)\|_{M(\gamma(s))} ds. \quad (9)$$

A minimizer is called a geodesic γ^* (with γ_s^*), which we assume to exist (cf. [33] for corresponding conditions). Integration of the local feedback $K(x)$ along the geodesic γ^* yields the input γ^u , and the feedback law κ :

$$\begin{aligned} \gamma^u(s) &:= v + \int_0^s K(\gamma^*(\tilde{s}))\gamma_s^*(\tilde{s})d\tilde{s}, \\ \kappa(x, z, v) &:= \gamma^u(1). \end{aligned} \quad (10)$$

The following proposition summarizes the properties of V_δ and κ .

Proposition 2 *Suppose Assumption 1 holds. Consider some $(x, z, v) \in \mathbb{R}^n \times \mathbb{R}^n \times \mathbb{R}^m$ such that for all $s \in [0, 1]$ it holds that $(\gamma^*(s), \gamma^u(s)) \in \mathbb{Z}$. Then, for all $\theta, \bar{\theta} \in \Theta_0$, and all $d \in \mathbb{D}$, the following inequalities hold:*

$$\|x - z\|_{\underline{M}} \leq V_\delta(x, z) \leq \|x - z\|_{\overline{M}}, \quad (11a)$$

$$\begin{aligned} \dot{V}_\delta(x, z) &= \frac{\partial V_\delta}{\partial x} \Big|_{(x, z)} \dot{x} + \frac{\partial V_\delta}{\partial z} \Big|_{(x, z)} \dot{z} \\ &\leq - \left(\rho_c - L_{\mathbb{D}} - \sum_{k=1}^p L_{G, k} |\theta - \bar{\theta}|_k \right) V_\delta(x, z) \\ &\quad + \|G(z, v)(\theta - \bar{\theta}) + E(z)d\|_{M(z)}, \end{aligned} \quad (11b)$$

with $\dot{x} = f_w(x, \kappa(x, z, v), \theta, d)$, $\dot{z} = \bar{f}(z, v, \bar{\theta})$, V_δ, κ according to Equations (9), (10), and constants $L_{G, k} \geq 0$, $k \in \mathbb{I}_{[1, p]}$, $L_{\mathbb{D}} \geq 0$ according to (A.5) and (A.7) in the appendix.

The proof of this proposition is given in Appendix A. In the nominal setting, i.e., $\mathbb{D} = \{0\}$, $\theta = \bar{\theta}$, Proposition 2 ensures that V_δ is an incremental Lyapunov function for $\dot{x} = f(x, u, \theta)$ with feedback $\kappa(x, z, v)$, analogous to [33]. The effect of the disturbance d and the parametric uncertainty $\theta - \bar{\theta}$ is suitably bounded with the constants $L_{\mathbb{D}}$, $L_{G, k}$ modifying the contraction rate ρ_c , and the model mismatch $\|G(z, v)(\theta - \bar{\theta}) + E(z)d\|_{M(z)}$ evaluated at the nominal trajectory. In the next section, we demonstrate that the condition $(\gamma^*(s), \gamma^u(s)) \in \mathbb{Z}$, $s \in [0, 1]$ is intrinsically satisfied by the proposed tube MPC and derive the tube dynamics based on Inequality (11b).

Remark 3 *The offline computation of matrices M, K satisfying Assumption 1 can be cast as linear matrix inequalities (LMIs), or a sum of squares (SOS) problem, using the convex re-parametrization $W = M^{-1}$ and $Y = KW$, compare [33, 42, 48, 51] for details. The geodesic γ^* is used in Equations (9) and (10) and can be computed using the Chebyshev global pseudospectral method with a suitable discretization [23].*

PROOF. First, note that (13e) holds at time $t = 0$ due to Condition (13c). For contradiction, suppose that there exists a time $\tau \geq 0$, such that (13e) holds for all $t \in [0, \tau]$, but is violated for $t > \tau$, i.e., $V_\delta(x(\tau), z_\tau) = \delta_\tau$ and $\dot{V}_\delta(x(\tau), z_\tau) > \dot{\delta}_\tau$. Given that (13e) holds for $t = \tau$, then Proposition 5 in combination with (13a) implies $(\gamma^*(s), \gamma^u(s)) \in \mathbb{Z}$, $s \in [0, 1]$, with $\gamma^* \in \Gamma(z_\tau, x(\tau))$, γ^u based on Equations (9) and (10). Hence, we can invoke Inequality (11b) in Proposition 2, yielding

$$\begin{aligned} \dot{V}_\delta(x(\tau), z_\tau) &\stackrel{(11b),(13d)}{\leq} f_\delta(V_\delta(x(\tau), z_\tau), z_\tau, v_\tau, \Theta_0, \bar{\theta}) \\ &= f_\delta(\delta_\tau, z_\tau, v_\tau, \Theta_0, \bar{\theta}) \stackrel{(13d)}{=} \dot{\delta}_\tau, \end{aligned}$$

which yields a contradiction. Hence, (13e) holds for $t \geq 0$. Furthermore, Proposition 5 and Inequality (13a) imply Inequality (13f). \square

Theorem 6 is applicable if the nominal trajectories z_t, v_t and the tube scaling δ_t are computed according to Conditions (13a)–(13d). In that case, all uncertain trajectories $x(t)$, with feedback $\kappa(x(t), z_t, v_t)$ are confined within the tube \mathbb{T}_t given by (5) (cf. Eq. (13e)) and satisfy the constraints (cf. Eq. (13f)). Thus, we obtained simpler sufficient conditions (cf. Eq. (13a)–(13d)) to compute a feasible solution to Problem (4).

3.3 Parameter update using set-membership estimation

We use set-membership estimation to update the polytopic parameter set Θ_0 online. This method is widely used in related RAMPC schemes [16, 17, 26, 28, 30], since it allows for reduced conservatism.

For the considered continuous-time setting, we assume that the state $x(t)$ and input $u(t)$ can be measured exactly, and a noisy measurement of the state derivative is available, i.e., $\hat{x}(t) = \dot{x}(t) + \epsilon(t)$, where $\epsilon(t) \in \mathbb{D}_\epsilon$, $t \geq 0$, with some polytope \mathbb{D}_ϵ . Then, the non-falsified parameter set given (x, u, \hat{x}) at time t is computed as

$$\begin{aligned} \Delta_t := \{ \theta \in \mathbb{R}^p \mid \exists (d, \epsilon) \in \mathbb{D} \times \mathbb{D}_\epsilon : \hat{x}(t) = \dot{x}(t) + \epsilon, \\ \dot{x}(t) = f_w(x(t), u(t), \theta, d) \}. \end{aligned}$$

We update the parameter set at each sampling time t_k , $k \in \mathbb{I}_{\geq 1}$ using $n_m \in \mathbb{I}_{\geq 1}$ measurements between t_{k-1} and t_k , using the following polytopic set-intersection:

$$\Theta_{t_k} = \Theta_{t_{k-1}} \cap_{j \in \mathbb{I}_{[0, n_m-1]}} \Delta_{t_{k-1} + j \frac{T_s}{n_m}}, \quad k \in \mathbb{I}_{\geq 1}. \quad (14)$$

Proposition 7 *The set Θ_{t_k} computed according to (14) is a polytope, which satisfies*

$$\theta \in \Theta_{t_k} \subseteq \Theta_{t_{k-1}} \subseteq \Theta_0, \quad k \in \mathbb{I}_{\geq 1}. \quad (15)$$

PROOF. Since $\Theta_{t_{k-1}}, \mathbb{D}$, and \mathbb{D}_ϵ are polytopes, the sets Δ_t , $t \geq 0$ are polyhedrons, and hence Θ_{t_k} , $k \in \mathbb{I}_{\geq 1}$ are also polytopes. The condition $\theta \in \Theta_{t_k} \subseteq \Theta_{t_{k-1}}$ follows for all $k \in \mathbb{I}_{\geq 1}$ recursively, using the fact that $\theta \in \Theta_0$, and the definition of the non-falsified sets Δ_t . \square

In contrast to existing nonlinear RAMPC schemes with set-membership estimation [17, 26], the presented framework allows for the general update of the uncertainty set (cf. Eq. (14)) without further restrictions. Also note that the set Θ_{t_k} is non-increasing, but may not converge to $\{\theta\}$ in general. Sufficient conditions for convergence can be found in [30, Cor. 8], assuming persistence of excitation and tight characterization of the disturbance bound.

Remark 8 *Computing the intersection of finitely many polytopes in (14) is straightforward. However, the number of facets and vertices of the parameter set Θ_{t_k} might grow with the updates leading to increasing computational complexity. This issue can be addressed by considering fixed-complexity polytopes of the form $\Theta_{t_k} = \{\theta \in \mathbb{R}^p \mid H\theta \leq h_{t_k}\}$, with some fixed matrix $H \in \mathbb{R}^{n_p \times p}$, and only update the vector $h_{t_k} \in \mathbb{R}^{n_p}$. This update retains the theoretical properties (15) and can be formulated as a linear program, see [28].*

Remark 9 *A noisy derivative \hat{x} can be obtained using suitable filters [1, 12, 26]. Equivalently, the non-falsified set can be written using an integral form [7, Eq. (17)]. Note that instead of set-membership estimation, the parameter sets Θ_t can, e.g., also be updated using Lyapunov-type arguments [1, 12] as long as Condition (15) remains valid.*

3.4 Terminal set constraint

In order to derive recursive feasibility and convergence guarantees of the proposed MPC scheme, we require the following standard conditions on the terminal ingredients (terminal set, terminal control law, terminal cost). In Proposition 11 below, we also propose a simple constructive design using a terminal equality constraint that satisfies these conditions.

Assumption 10 *There exists a terminal set $\mathbb{X}_f \subseteq \mathbb{R}^n \times \mathbb{R}_{\geq 0} \times \Theta_0 \times 2^{\mathbb{R}^p}$, a terminal control law $k_f : \mathbb{R}^n \times \Theta_0 \rightarrow \mathbb{R}^m$, and a continuous terminal cost $\ell_f : \mathbb{R}^n \times \Theta_0 \rightarrow \mathbb{R}_{\geq 0}$, such that for any $(z, \delta, \bar{\theta}, \Theta) \in \mathbb{X}_f$, the trajectories $\dot{z}_\tau = \bar{f}(z_\tau, k_f(z_0, \bar{\theta}), \bar{\theta})$, $\dot{\delta}_\tau = f_\delta(\delta_\tau, z_\tau, k_f(z_0, \bar{\theta}), \Theta, \bar{\theta})$, $\tau \in [0, T_s]$, with $\delta_0 = \delta$, $z_0 = z$ satisfy*

- *positive invariance:*

$$(z_{T_s}, \delta_{T_s}, \bar{\theta}, \Theta) \in \mathbb{X}_f, \quad (16a)$$

- *constraint satisfaction:*

$$h_j(z_\tau, k_f(z_0, \bar{\theta})) + c_j \delta_\tau \leq 0, \quad j \in \mathbb{I}_{[1,r]}, \quad \tau \in [0, T_s], \quad (16b)$$

- *local control Lyapunov function:*

$$\int_0^{T_s} \ell(z_\tau, k_f(z_0, \bar{\theta}), \bar{\theta}) d\tau \leq \ell_f(z_0, \bar{\theta}) - \ell_f(z_{T_s}, \bar{\theta}). \quad (16c)$$

Furthermore, for any $\hat{\delta} \in [0, \delta]$, $\hat{\Theta} \subseteq \Theta$, it holds

$$(z, \delta, \bar{\theta}, \Theta) \in \mathbb{X}_f \Rightarrow (z, \hat{\delta}, \bar{\theta}, \hat{\Theta}) \in \mathbb{X}_f. \quad (16d)$$

The requirements (16a)-(16c) are comparable to the standard conditions in MPC (cf. [40]). Furthermore, we pose the monotonicity property (16d). The terminal control input is chosen to be constant in the interval $[0, T_s]$, which ensures that a piece-wise constant input parametrization can be used in the MPC. The following proposition shows that these conditions hold using a simple terminal equality constraint w.r.t. the desired steady-state (cf. Sec. 2.2).

Proposition 11 *Suppose Assumption 1 holds. Then, Assumption 10 is satisfied with $k_f(z, \bar{\theta}) = v_{\text{ref}}(\bar{\theta})$, $\ell_f(z, \bar{\theta}) \equiv 0$, and the following terminal set:*

$$\mathbb{X}_f = \left\{ (z, \delta, \bar{\theta}, \Theta) \in \mathbb{R}^n \times \mathbb{R}_{\geq 0} \times \Theta_0 \times 2^{\mathbb{R}^p} \right\} \quad (17a)$$

$$z = z_{\text{ref}}(\bar{\theta}), \quad (17b)$$

$$\exists \bar{\delta}_f \in \mathbb{R}_{\geq 0} : \delta \in [0, \bar{\delta}_f], \quad (17c)$$

$$f_\delta(\bar{\delta}_f, z, k_f(z, \bar{\theta}), \Theta, \bar{\theta}) \leq 0, \quad (17d)$$

$$h_j(z, k_f(z, \bar{\theta})) + c_j \bar{\delta}_f \leq 0, \quad \forall j \in \mathbb{I}_{[1,r]}. \quad (17e)$$

PROOF. Condition (17b) along with the choice of k_f yields $z_\tau = z_{\text{ref}}(\bar{\theta})$ for $\tau \in [0, T_s]$. Furthermore, $\delta_0 \in [0, \bar{\delta}_f]$ (cf. (17c)) and Inequality (17d) yields $\delta_\tau \in [0, \bar{\delta}_f]$, $\tau \in [0, T_s]$. Hence, positive invariance (16a) follows by considering the same $\bar{\delta}_f$. Moreover, Condition (17e) and $\delta_\tau \in [0, \bar{\delta}_f]$, $\tau \in [0, T_s]$ yield Inequality (16b). Condition (16c) follows with $\ell(z_\tau, k_f(z_0, \bar{\theta}), \bar{\theta}) = 0$ using (7). The monotonicity property (16d) follows using Condition (17c) and the definition of f_δ (13d) yielding $f_\delta(\bar{\delta}_f, z, k_f(z, \bar{\theta}), \hat{\Theta}, \bar{\theta}) \leq f_\delta(\bar{\delta}_f, z, k_f(z, \bar{\theta}), \Theta, \bar{\theta}) \leq 0$, $\hat{\Theta} \subseteq \Theta$. \square

Invariance of the terminal set w.r.t. the nominal dynamics f is guaranteed by requiring the terminal state to coincide with the steady-state of the nominal dynamics z_{ref} (17b) and using the corresponding input v_{ref} as the terminal control law. Note that the terminal set constraint includes not only the nominal state z , but also

the tube scaling δ , the nominal parameter $\bar{\theta}$, and the parameter set Θ , since Θ is updated online and $\delta, \bar{\theta}$ are optimization variables in the proposed RAMPC framework (Sec. 3.5). Positive invariance (cf. (17d)) and constraint satisfaction (cf. (17e)) are shown by additionally computing a constant $\bar{\delta}_f \geq 0$ that upper bounds the tube scaling δ in the terminal set. For implementation, the constant $\bar{\delta}_f \geq 0$ needs to be included as a decision variable in the MPC optimization problem introduced below.

3.5 RAMPC framework and theoretical analysis

In the following, we present the overall RAMPC algorithm (Alg. 1-2), including a corresponding theoretical analysis of the closed-loop properties (Thm. 12). The RAMPC scheme approximates the solution to the infinite-horizon Problem (4) by a finite prediction horizon $T_f = T_s N$, $N \in \mathbb{I}_{\geq 1}$ using a receding horizon implementation with a sampling period of T_s . In particular, at time t , given the measured state $x(t)$ and the updated parameter set Θ_t , the proposed RAMPC scheme is characterized by the following optimization problem:

$$\begin{aligned} V_{T_f}^*(x(t), \Theta_t) &= \min_{\substack{v_{\cdot|t}, z_{\cdot|t} \\ \delta_{\cdot|t}, \bar{\theta}_t}} \int_0^{T_f} \ell(z_\tau|t, v_\tau|t, \bar{\theta}_t) d\tau + \ell_f(z_{T_f|t}, \bar{\theta}_t) \\ \text{s.t.} \quad \dot{z}_\tau|t &= \bar{f}(z_\tau|t, v_\tau|t, \bar{\theta}_t), & (18a) \\ \dot{\delta}_\tau|t &= f_\delta(\delta_\tau|t, z_\tau|t, v_\tau|t, \Theta_t, \bar{\theta}_t), & (18b) \\ \bar{\theta}_t &\in \Theta_0, & (18c) \\ h_j(z_\tau|t, v_\tau|t) + c_j \delta_\tau|t &\leq 0, & (18d) \\ V_\delta(x(t), z_{0|t}) &\leq \delta_{0|t}, & (18e) \\ (z_{T_f|t}, \delta_{T_f|t}, \bar{\theta}_t, \Theta_t) &\in \mathbb{X}_f, & (18f) \\ \tau &\in [0, T_f], \quad j \in \mathbb{I}_{[1,r]}. \end{aligned}$$

The decision variables are the nominal state and input trajectories $z_{\cdot|t}, v_{\cdot|t}$, the tube scaling $\delta_{\cdot|t}$, and the nominal parameter $\bar{\theta}_t$. The tube scaling $\delta_{\tau|t}$ is propagated according to Theorem 6 (cf. (18b), (18e)) and the nominal trajectory $z_{\tau|t}$ satisfies the nominal dynamics \bar{f} (18a). The constraint tightening (18d) ensures that the true state and input trajectory satisfy the constraints (2) (cf. Prop. 5 and Thm. 6). Condition (18c) allows to additionally optimize over the nominal parameter that influences the dynamics in (18a)–(18b). Furthermore, Condition (18f) captures the terminal constraint. For simplicity, we parameterize the nominal input $v_\tau|t$ as piece-wise constant in each interval $\tau \in [jT_s, (j+1)T_s)$, $j \in \mathbb{I}_{[0, N-1]}$.

Appropriate conditions ensuring that a minimizer to Problem (18) exists can be found in [9, Prop. 2]. We assume that a corresponding unique minimizer exists, which is denoted by the superscript \star . We solve the problem at each sampling time t_k , $k \in \mathbb{I}_{\geq 0}$, and the resulting

closed-loop system is given by

$$\begin{aligned} u(t) &= \kappa(x(t), z_{t-t_k|t_k}^*, v_{t-t_k|t_k}^*), \quad t \in [t_k, t_{k+1}), \\ \dot{x}(t) &= f_w(x(t), u(t), \theta, d(t)). \end{aligned} \quad (19)$$

The offline design and the online operation are captured in the algorithms below.

Algorithm 1 Offline design

- Given model with uncertainty characterization \mathbb{D} , Θ_0 , \mathbb{D}_e , constraints (2), desired setpoint $z_{\text{ref}}(\bar{\theta})$, $v_{\text{ref}}(\bar{\theta})$ and stage cost weighting $Q, R \succeq 0$ (7).
- 1: Compute $M(x)$, $K(x)$ and ρ_c (Asm. 1, Rk. 3).
 - 2: Compute constants $L_{\mathbb{D}}$ (A.7), $L_{G,k}$ (A.5), c_j (12b).
 - 3: Set sampling period T_s and prediction horizon T_f .
 - 4: Design terminal ingredients (Asm. 10, Prop. 11).
-

Algorithm 2 Online operation

- for** each sampling time $t_k = kT_s$, $k \in \mathbb{I}_{\geq 0}$ **do**
 Update Θ_{t_k} (14) using measurements (x, \dot{x}, u) .
 Solve Problem (18).
 Apply feedback κ over period $t \in [t_k, t_{k+1})$ (19).
end for
-

The following theorem summarizes the theoretical properties of the proposed RAMPC algorithm.

Theorem 12 *Let Assumptions 1 and 10 hold. Suppose that Problem (18) is feasible at time $t = 0$ with initial state x_0 and parameter set Θ_0 . Then, Problem (18) is feasible for all sampling times t_k , $k \in \mathbb{I}_{\geq 0}$, and the closed-loop system (19) resulting from Algorithm 2 satisfies the constraints (2) for all $t \geq 0$. Furthermore, the resulting nominal trajectories converge to the reference state and input, i.e., $\lim_{k \rightarrow \infty} \left\| (z_{\tau|t_k}^*, v_{\tau|t_k}^*) - (z_{\text{ref}}(\bar{\theta}_{t_k}^*), v_{\text{ref}}(\bar{\theta}_{t_k}^*)) \right\| = 0$, $\tau \in [0, T_s]$.*

PROOF. Part I: Assume that Problem (18) is feasible at some time t_k , $k \in \mathbb{I}_{\geq 0}$. For simplicity, we define $v_{\tau|t_k}^* := k_f(z_{T|t_k}^*, \bar{\theta}_{t_k}^*)$ and $z_{\tau|t_k}^*$, $\delta_{\tau|t_k}^*$ according to (18a) and (18b) for $\tau \in [T_f, T_f + T_s]$. At time t_{k+1} , consider the candidate solution

$$\begin{aligned} \bar{\theta}_{t_{k+1}} &= \bar{\theta}_{t_k}^* \in \Theta_0, \quad v_{\tau|t_{k+1}} = v_{\tau+T_s|t_k}^*, \quad \tau \in [0, T_f], \\ z_{0|t_{k+1}} &= z_{T_s|t_k}^*, \quad \delta_{0|t_{k+1}} = V_{\delta}(x(t_{k+1}), z_{T_s|t_k}^*), \end{aligned}$$

with trajectories $z_{\tau|t_{k+1}}$, $\delta_{\tau|t_{k+1}}$, $\tau \in (0, T_f]$ according to the constraints (18a), (18b), which implies $z_{\tau|t_{k+1}} = z_{\tau+T_s|t_k}^*$, $\tau \in [0, T_f]$. In the following, we show that the tube scaling satisfies the following nestedness property:

$$\delta_{\tau|t_{k+1}} \leq \delta_{\tau+T_s|t_k}^*, \quad \tau \in [0, T_f]. \quad (20)$$

First, note that Condition (13e) in Theorem 6 also holds for any $\Theta \subseteq \Theta_0$ with $\dot{x} = f_w(x, u, \theta, d)$, $\dot{\delta} = f_{\delta}(\delta, z, v, \Theta, \bar{\theta})$, $\bar{\theta} \in \Theta_0$, $\theta \in \Theta$, $d \in \mathbb{D}$ yielding

$$V_{\delta}(x(t_k + \tau), z_{\tau|t_k}^*) \leq \delta_{\tau|t_k}^*, \quad \tau \in [0, T_s].$$

Hence, the initial value of the tube scaling satisfies

$$\delta_{0|t_{k+1}} = V_{\delta}(x(t_{k+1}), z_{T_s|t_k}^*) \leq \delta_{T_s|t_k}^*.$$

For contradiction, suppose that there exists a time $\hat{\tau} \in [0, T_f]$, such that (20) holds for all $\tau \in [0, \hat{\tau}]$, but is violated for $\tau > \hat{\tau}$, i.e., $\delta_{\hat{\tau}|t_{k+1}} = \delta_{\hat{\tau}+T_s|t_k}^*$ and $\delta_{\hat{\tau}|t_{k+1}} > \delta_{\hat{\tau}+T_s|t_k}^*$. The dynamics of the tube scaling (13d) in combination with $\Theta_{t_{k+1}} \subseteq \Theta_{t_k}$ yield

$$\begin{aligned} \dot{\delta}_{\hat{\tau}|t_{k+1}} &= f_{\delta}(\delta_{\hat{\tau}|t_{k+1}}, z_{\hat{\tau}+T_s|t_k}^*, v_{\hat{\tau}+T_s|t_k}^*, \Theta_{t_{k+1}}, \bar{\theta}_{t_k}^*) \\ &\leq f_{\delta}(\delta_{\hat{\tau}+T_s|t_k}^*, z_{\hat{\tau}+T_s|t_k}^*, v_{\hat{\tau}+T_s|t_k}^*, \Theta_{t_k}, \bar{\theta}_{t_k}^*) \\ &= \dot{\delta}_{\hat{\tau}+T_s|t_k}^*, \end{aligned}$$

which is a contradiction, and hence (20) holds.

The candidate solution satisfies Condition (18f) due to the invariance (16a) and monotonicity property (16d) of \mathbb{X}_f , using Inequality (20) and $\Theta_{t_{k+1}} \subseteq \Theta_{t_k}$. Inequality (18d) for $\tau \in [T_f - T_s, T_f]$ follows analogously using Condition (16b). For $\tau \in [0, T_f - T_s]$, Condition (18d) holds with:

$$\begin{aligned} h_j(z_{\tau|t_{k+1}}, v_{\tau|t_{k+1}}) + c_j \delta_{\tau|t_{k+1}} & \\ \stackrel{(20)}{\leq} h_j(z_{\tau+T_s|t_k}^*, v_{\tau+T_s|t_k}^*) + c_j \delta_{\tau+T_s|t_k}^* & \stackrel{(18d)}{\leq} 0, \end{aligned}$$

where we used feasibility of Problem (18) at time t_k and the fact that $c_j \geq 0$.

Part II: Constraint satisfaction (2) for the closed-loop system follows from Theorem 6 using the tightened constraints (18d) for $\tau \in [0, T_s]$ and the tube dynamics (18e), (18b).

Part III: Convergence is established using standard inequalities for the optimal cost $V_{T_f}^*$. In particular, the feasible candidate solution provides an upper bound to the optimal cost, i.e.,

$$\begin{aligned} &V_{T_f}^*(x(t_{k+1}), \Theta_{t_{k+1}}) \\ &\leq \int_0^{T_f} \ell(z_{\tau+T_s|t_k}^*, v_{\tau+T_s|t_k}^*, \bar{\theta}_{t_k}^*) + \ell_f(z_{T_f+T_s|t_k}^*, \bar{\theta}_{t_k}^*) d\tau \\ &= V_{T_f}^*(x(t_k), \Theta_{t_k}) - \int_0^{T_s} \ell(z_{\tau|t_k}^*, v_{\tau|t_k}^*, \bar{\theta}_{t_k}^*) d\tau \\ &\quad - \ell_f(z_{T_f|t_k}^*, \bar{\theta}_{t_k}^*) + \int_{T_f}^{T_f+T_s} \ell(z_{\tau|t_k}^*, v_{\tau|t_k}^*, \bar{\theta}_{t_k}^*) d\tau \\ &\quad + \ell_f(z_{T_f+T_s|t_k}^*, \bar{\theta}_{t_k}^*) \\ &\stackrel{(16c)}{\leq} V_{T_f}^*(x(t_k), \Theta_{t_k}) - \int_0^{T_s} \ell(z_{\tau|t_k}^*, v_{\tau|t_k}^*, \bar{\theta}_{t_k}^*) d\tau. \end{aligned}$$

Applying the previous inequality recursively yields

$$\begin{aligned} & V_{T_f}^*(x_0, \Theta_0) - \limsup_{k \rightarrow \infty} V_{T_f}^*(x(t_k), \Theta_{t_k}) \\ & \geq \sum_{k=0}^{\infty} \int_0^{T_s} \ell(z_{\tau|t_k}^*, v_{\tau|t_k}^*, \bar{\theta}_{t_k}^*) d\tau. \end{aligned}$$

Compact constraints in combination with a continuous cost imply a uniform bound on $V_{T_f}^*$, and hence the right hand side of the above inequality is bounded, yielding

$$\lim_{k \rightarrow \infty} \int_0^{T_s} \ell(z_{\tau|t_k}^*, v_{\tau|t_k}^*, \bar{\theta}_{t_k}^*) d\tau = 0.$$

Note that $z_{\tau|t_k}^*$ is uniformly continuous in τ , given \bar{f} Lipschitz and $(z_{\tau|t_k}^*, v_{\tau|t_k}^*, \bar{\theta}_{t_k}^*)$ subject to compact constraints (18d), (18c). Furthermore, $v_{\tau|t_k}^*$ and $\bar{\theta}_{t_k}^*$ are constant on $\tau \in [0, T_s)$, thus $\ell(z_{\tau|t_k}^*, v_{\tau|t_k}^*, \bar{\theta}_{t_k}^*)$ is uniformly continuous on $\tau \in [0, T_s)$. Since ℓ is also positive definite, Barbalat's Lemma [15] can be invoked yielding:

$$\lim_{k \rightarrow \infty} \left\| (z_{\tau|t_k}^*, v_{\tau|t_k}^*) - (z_{\text{ref}}(\bar{\theta}_{t_k}^*), v_{\text{ref}}(\bar{\theta}_{t_k}^*)) \right\| = 0. \quad \square$$

Theorem 12 provides all the desired properties of a robust MPC scheme, while incorporating online updates of the parameter set Θ_t to reduce conservatism.

Remark 13 *The dynamics (18b) involve the maximization operator from f_δ (13d), which may complicate integration. This issue is circumvented by introducing an auxiliary variable $\bar{w}_\tau|t \geq 0$ and using the following constraints:*

$$\begin{aligned} \dot{\delta}_\tau|t &= -(\rho_c - L_D)\delta_\tau|t + \bar{w}_\tau|t, \\ \bar{w}_\tau|t &\geq \sum_{k=1}^p L_{G,k} |\theta^i - \bar{\theta}_t|_k |\delta_\tau|t + \|G(z_\tau|t, v_\tau|t)(\theta^i - \bar{\theta}_t) \\ &\quad + E(z_\tau|t)d^j\|_{M(z_\tau|t)}, \quad i \in \mathbb{I}_{[1, n_{\Theta_t}]}, \quad j \in \mathbb{I}_{[1, n_D]}. \end{aligned} \quad (21)$$

Hence, we can equivalently write the dynamics (18a), (18b) and the constraints (18d) using smooth continuous-time dynamics with state $(z, \delta) \in \mathbb{R}^{n+1}$, input $(v, \bar{w}) \in \mathbb{R}^{m+1}$, and continuous-time constraints (18d), (21), analogous to standard continuous-time MPC schemes [11, Fig. 12.10]. Correspondingly, we use standard methods to integrate the dynamics. Furthermore, we relax the continuous-time constraint satisfaction by only enforcing constraints on some discrete points [40, Sec. 8]. However, one could also use additional modifications to rigorously guarantee continuous-time constraint satisfaction (cf. [32, Thm. 3], [10]).

Note that constraint (18e) on the initial state can be

equivalently written as $\int_0^1 \|\gamma_s(s)\|_{M(\gamma(s))} ds \leq \delta_{0|t}$ (cf. Eq. (9)) by using the curve $\gamma \in \Gamma(z_{0|t}, x(t))$ as an additional optimization variable. The integral is approximated with numerical quadrature, and the curve γ is finitely parametrized using a pseudospectral method (cf., Remark 3 and [23, 51]). Thus, Problem (18) is approximated with a finite dimensional nonlinear program.

3.6 Discussion

In the following, we discuss the results and benefits of the proposed RAMPC framework in comparison to existing robust and robust adaptive MPC schemes.

Stability properties: Suppose for simplicity that $z_{\text{ref}}(\bar{\theta})$, $v_{\text{ref}}(\bar{\theta})$ is unique. Then, the convergence result in Theorem 12 yields that the uncertain closed-loop trajectory $x(t)$ converges to an RPI set corresponding to the stabilizing feedback $u(t) = \kappa(x(t), z_{\text{ref}}(\bar{\theta}), v_{\text{ref}}(\bar{\theta}))$, analogous to standard tube MPC results [3, 34]. To improve performance, the cost function can also be based on a state trajectory predicted according to the true measured state $x(t)$ and some other parameter estimate $\hat{\theta}_{t_k}$. Specifically, by using least mean square estimate, finite-gain \mathcal{L}_2 -stability w.r.t. disturbance d is shown in [16, 17, 28].

Tube propagation: The tube propagation derived in Theorem 6 is similar to the RMPC formulations presented in [20, App. B] and [17], which use the same tube parametrization (5) with V_δ , z , δ , compare also [39]. However, in [17, 20] explicit design formulas for the tube propagation were only established for the special case of ellipsoidal sets (cf. [17, Sec. 3.5]) and [39] only studies the special case of a shift invariant parametrization.² Furthermore, the simple tube propagation in [1, 12, 37] based on Lipschitz continuity is a further special case of the proposed framework with $M(z) = I$ and $K(z) = 0$, compare also [20, Rk. 4] and [17, Sec. 3.6] for a detailed discussion. In contrast to these existing RMPC approaches, we utilized general CCMs to provide simple explicit formulas for the tube dynamics and constraint tightening using the gradient theorem, compare (A.5), (A.7), (12b).

By using the upper bound $M(z) \preceq \bar{M}$ in Inequality (21), we can also obtain a computationally cheaper, yet more conservative result. Moreover, in the robust case ($\bar{\theta}$, Θ constant), we can compute a constant $L \leq L_D + \max_{i \in \mathbb{I}_{[1, n_{\Theta_0}]}} \sum_{k=1}^p L_{G,k} |\theta^i - \bar{\theta}|_k$, which is also less conservative compared to the formulation in [20].

Homothetic vs. rigid tube: Many robust MPC formulations use a fixed (rigid) tube scaling $\delta_\tau|t = \bar{\delta} > 0$ for all

² The controller κ , the incremental Lyapunov function V_δ , the tube \mathbb{T} , and the bound on the model mismatch may only depend on the error $x - z$, which excludes general CCMs.

$\tau \geq 0$ instead of implementing a tube propagation of the form Eq. (13d), compare [3, 42, 43, 46, 49, 51]. This special case can be recovered by computing a constant $\bar{\delta} > 0$, such that $\delta = f_\delta(\bar{\delta}, z, v, \bar{\theta}, \Theta) \leq 0$ for all $(z, v) \in \mathbb{Z}$. Similarly, an arbitrary constant $\delta_{\tau|t} = \bar{\delta}_{\max} > 0$, $\tau \geq 0$, can be fixed offline by adding the constraint $\bar{w}_{\tau|t} \leq \bar{w}_{\max} := (\rho_c - L_{\mathbb{D}})\bar{\delta}_{\max}$ to upper bound the right hand side of Inequality (21) to the optimization problem. This restricts the nominal state and input to regions with small uncertainty, compare [46]. On the other hand, the proposed homothetic tube MPC overcomes this conservatism by systematically changing the scaling δ along the horizon, compare also the numerical example in Section 4.

Initial state constraint: The proposed homothetic tube MPC framework allows for an optimization over the initial state $z_{0|t}$. However, this requires an evaluation of V_δ in Condition (18e), which increases the computational complexity, compare Remark 13. This can be avoided by considering the more restrictive initial state constraint $z_{0|t} = x(t)$, $\delta_{0|t} = 0$ (cf. Eq. (18e)). Such an initial state constraint is also suggested in the homothetic tube MPC schemes in [17, 20], where recursive feasibility is demonstrated using a candidate input v that tracks the previous optimal solution z^* .³ We note that this approach necessitates a stronger (robust) positive invariance condition on the terminal set, which excludes the simple terminal equality constraints (cf. Prop. 11).

Adaptive MPC: In the following, we discuss the difference in how we utilize set-membership estimation compared to existing adaptive MPC frameworks [1, 12, 17, 26]. One main novelty in our work is the optimization over the nominal parameter $\bar{\theta}_t$, yielding a number of benefits. Intuitively, one might be inclined to simply fix $\bar{\theta}_t$ at the center of Θ_t , as done in [1, 8, 12, 16, 17, 26], since this results in small tube scaling δ_t (cf. Eq. (13d)). However, this complicates the recursive feasibility analysis, limiting the applicability to restrictive parameter sets, such as hypercubes [8, 16, 17, 26] or balls [1, 12]. On the other hand, optimizing over $\bar{\theta}_t$ enables a simple recursive feasibility proof by shifting the previous optimal solution. As a result, the proposed RAMPC scheme is applicable to general CCMs (Asm. 1), and requires no restrictions on the parametrization in the set-membership estimation (Sec. 3.3).

Finally, in contrast to existing adaptive methods (cf. [16, App. B], [8, Chap. II.D]), tracking parameter dependent set-points $(z_{\text{ref}}(\bar{\theta}), v_{\text{ref}}(\bar{\theta}))$ is straightforward. Such a set-point can be implicitly specified using:

$$(z_{\text{ref}}(\bar{\theta}), v_{\text{ref}}(\bar{\theta})) \in \arg \min_{\substack{z \in \mathbb{R}^n \\ v \in \mathbb{R}^m}} \|Cz + Dv - y^d\|^2 \\ \text{s.t. } \bar{f}(z, v, \bar{\theta}) = 0, \quad (z, v) \in \mathbb{Z},$$

³ Accounting for the piece-wise constant input parametrization requires additional modifications (cf., e.g., [20, Rk. 14]).

where y^d is a reference for a system output $y = Cx + Du$. This optimization problem can also be included in the MPC formulation, similar to [24].

4 Numerical example

The following example demonstrates the benefits of the proposed homothetic tube MPC framework and the on-line model updates. We consider the following planar quadrotor from [43, 51]:

$$\begin{bmatrix} \dot{p}_1 \\ \dot{p}_2 \\ \dot{\phi} \\ \dot{v}_1 \\ \dot{v}_2 \\ \ddot{\phi} \end{bmatrix} = \begin{bmatrix} v_1 \cos(\phi) - v_2 \sin(\phi) \\ v_1 \sin(\phi) + v_2 \cos(\phi) \\ \dot{\phi} \\ v_2 \dot{\phi} - g \sin(\phi) \\ -v_1 \dot{\phi} - g \cos(\phi) \\ 0 \end{bmatrix} + \begin{bmatrix} 0 & 0 \\ 0 & 0 \\ 0 & 0 \\ 0 & 0 \\ \frac{1}{m} & \frac{1}{m} \\ \frac{l}{J} & \frac{-l}{J} \end{bmatrix} u + \begin{bmatrix} 0 \\ 0 \\ 0 \\ \cos(\phi) \\ -\sin(\phi) \\ 0 \end{bmatrix} d,$$

where p_1, p_2 are horizontal and vertical positions, v_1, v_2 are velocities in the body frame, and $\phi, \dot{\phi}$ denote the angle/angular velocity. The control input $u = [u_1, u_2]^T$ is the thrust force produced by the propellers and d is a wind disturbance. Furthermore, g, m , and l denote the gravitational acceleration, mass, and the distance between each of the propellers and the vehicle center, respectively. Compared to the setting in [43, 51], we additionally consider the mass as an uncertain parameter $\theta = \frac{1}{m}$ with initial estimate $\bar{\theta}_0 = 2.058$, uncertainty set $\Theta_0 = [0.99\bar{\theta}_0, 1.01\bar{\theta}_0]$, and true parameter $\theta = 1.01\bar{\theta}_0$. The disturbance satisfies $d(t) \in \mathbb{D} := [-0.1, 0.1]$. The state and input constraint set (3) are given by: $|\phi| \leq \pi/3$, $|\dot{\phi}| \leq \pi$, $|v_1| \leq 2$, $|v_2| \leq 1$, $u_i \in [-1, 3.5]$, $i \in \{1, 2\}$. The goal is to reach position $p = 0$, which corresponds to $z_{\text{ref}}(\bar{\theta}) = 0$, $v_{\text{ref}}(\bar{\theta}) = \frac{g}{2\bar{\theta}}[1, 1]^T$. We have placed circular obstacles between the initial position and the goal in order to provide a challenging control problem, compare Figures 1 and 3. Note that planning robust trajectories in this cluttered environment requires small tubes, which is only attainable with a relatively small uncertainty sets \mathbb{D}, Θ_0 . Handling significantly larger uncertainty with the proposed framework would lead to feasibility issues. Nonetheless, the proposed approach is significantly less conservative than existing methods [43, 51] as shown in the subsection *Comparison to rigid tube MPC* below.

Remark 14 Applying the presented RAMPC scheme for any system is straightforward in case a valid CCM is available. This includes any feedback linearizable system (cf. [33]) or any system that is quadratically stabilizable, i.e., admits a constant CCM. In particular, CCMs have been derived for a large class of nonlinear systems in the literature, including e.g., 3D quadrotors [51], cars [6, 18], manipulators [6], and chemical reactors [18].

Implementation details

The CCM (Asm. 1) is computed using the convex re-parametrization Y, W (cf. Remark 3) by adjusting the SOS code from [51]. We optimize for a CCM that results in a smaller tube by adding the following LMI

$$\begin{bmatrix} W & G\tilde{\theta} + Ed \\ (G\tilde{\theta} + Ed)^\top & \tilde{w}_{\max}^2 \end{bmatrix} \succeq 0, \quad \forall (d, \tilde{\theta} + \bar{\theta}_0) \in \mathbb{D} \times \Theta_0 \quad (22)$$

and minimizing \tilde{w}_{\max} .⁴ We note that simpler RMPC schemes based on ellipsoidal/polytopic RPI sets (cf., e.g., [39, 46, 49]), corresponding to constant matrices Y, W or feedback linearization (cf. [26]) are not feasible for this nonlinear problem. In particular, if the linearized model around an equilibrium would be used for a standard linear robust MPC design [5], then the constraint tightening on the horizontal position would be over 100 meters at the end of the prediction horizon, i.e., multiple factors too large to apply to the cluttered environment in Figure 1. This shows that the problem is in fact highly nonlinear and requires nonlinear robust MPC techniques to achieve good performance.

The dynamics (18a), (18b) as well as the true dynamics (1) are discretized using explicit Runge-Kutta 4 discretization with the sampling interval $T_s = 150$ ms, and we only enforce the state and input constraints at the sampling times t_k (cf. Remark 13). We choose a prediction horizon of $T_f = N \cdot T_s = 3.75$ s based on $N = 25$ steps. The disturbance $d(t)$ and the measurement noise $\epsilon(t)$ are sampled uniformly from the sets \mathbb{D} and $\mathbb{D}_\epsilon = \mathbb{D}$. The geodesic in (18e) is approximated using Chebyshev interpolating polynomials up to degree 2 (cf. Remark 13) with the code from [51].

All computations were carried out using Matlab, on a Dell Inspiron 15-3567 laptop with Intel i7-7500U CPU and 8 GB RAM running Windows 10. The MPC problems are solved with IPOPT [47] formulated in CasADi [2].⁵ The corresponding code is available online.⁶

Benefits of online model updates

We demonstrate the benefits of online model updates using set-membership estimation (cf. Sec. 3.3) by comparing the proposed robust adaptive MPC to a purely robust MPC variation that uses $\Theta_{t_k} = \Theta_0$. The results are shown in Figure 1. Given the initial uncertainty, we cannot plan a safe trajectory through the smaller gap between the obstacles. Hence, both formulations plan a

⁴ Applying the Schur complement to (22) yields $\tilde{w}_{\max}^2 \geq \|G\tilde{\theta} + Ed\|_M^2$ which provides an upper bound to the last term in f_δ (13d).

⁵ To avoid local minima, we solve the resulting NLP with initial guesses based on different paths around the obstacles.

⁶ gitlab.ethz.ch/ics/RAMPC-CCM

more conservative trajectory passing through the larger gap. After the first sampling period $t = T_s$, we perform the set-membership update (14) using $n_m = 1$, resulting in a 42% reduction of the size of the parameter set Θ_{t_k} . As a result, the adaptive formulation can plan through the smaller gap. As standard in (robust) MPC, the closed-loop trajectories can be significantly more aggressive than the conservative open-loop predictions due to the re-planning inherent in MPC. The evolution of the parameter set Θ_{t_k} in the simulation is depicted in Figure 2.

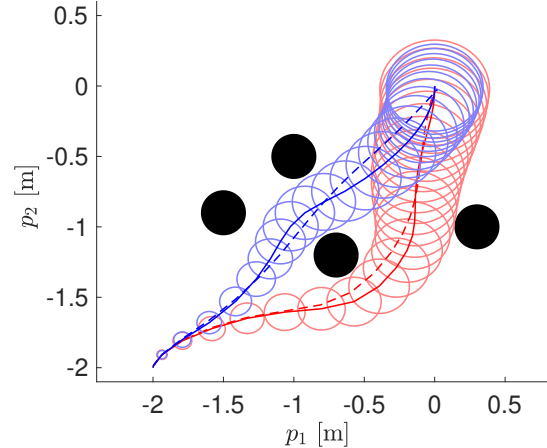


Fig. 1. Comparison of the proposed RMPC scheme with (blue) and without (red) adaptation. The open-loop solutions at $t = T_s$ are shown with nominal trajectories (solid) and ellipsoidal over-approximations of the tube based on \underline{M} . The closed-loop trajectories are dashed.

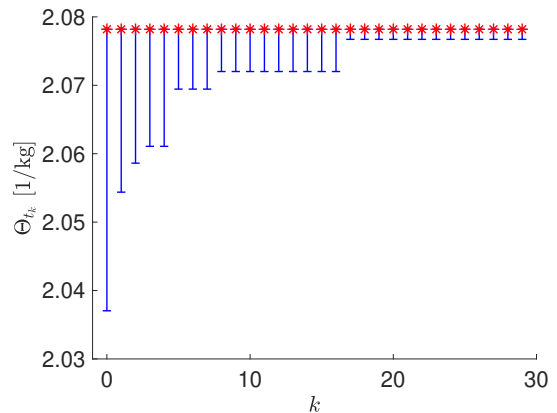


Fig. 2. Evolution of the uncertain parameter set Θ_{t_k} (blue intervals) over the simulation steps k . The true parameter value is indicated by the red stars.

Comparison to rigid tube MPC

We also show the advantages of the state and input dependent disturbance bound (13d) in the proposed homothetic tube MPC scheme compared to a rigid tube approach, which is widely used in literature [34, 42, 43,

49,51]. To this end, we focus on the purely robust setting and use no online model updates. We compute a constant scaling $\bar{\delta}$ to recover the rigid tube, compare Section 3.6. To ensure initial feasibility of this more conservative approach, we decrease the parametric uncertainty by 50% and increase the prediction horizon to $N = 35$ steps for both approaches. The resulting open-loop predictions and closed-loop trajectories can be seen in Figure 3. The rigid tube (red) is significantly larger and correspondingly the planned trajectory cannot pass between the obstacles, but bypasses them from the right. On the other hand, the proposed homothetic tube MPC formulation finds a feasible solution through the smaller gap between the obstacles, demonstrating improved flexibility.

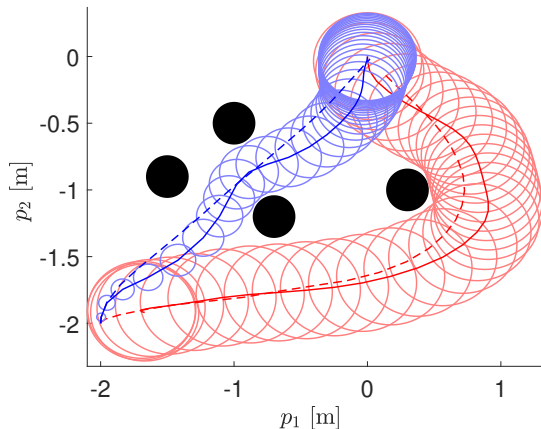


Fig. 3. Comparison of rigid tube MPC (red) and the proposed homothetic tube RMPC (blue). The open-loop solutions at $t = 0$ are shown with nominal trajectories (solid) and ellipsoidal over-approximations of the tube based on \underline{M} . The closed-loop trajectories are dashed.

Computational complexity

The offline computations to obtain the CCM and corresponding constants (Alg. 1) took 10 minutes, while the just-in-time compilation (jit, cf. [2]) of the RAMPC scheme took another 20 minutes. The following table lists the online computation times for one iteration in IPOPT for the considered MPC schemes with a prediction horizon of $N = 25$ steps.

RAMPC	RMPC	RMPC - Euler	Rigid tube	Nominal MPC
60.46 ms	54.64 ms	19.52 ms	8.79 ms	4.32 ms

As one can see, adaptation leads to a relatively small increase in computation time (around 10%) due to the additional variables $\bar{\theta}_t, \bar{\delta}_f$ that appear in constraints (18a)–(18c), (18f). We also included an RMPC scheme that uses an explicit Euler discretization for the tube propagation (18b). This simplification yields a significant reduction in computation times, yet the error in the tube propagation is below 5% over the full horizon. Finally,

the rigid tube approach has the lowest computational complexity among the RMPC frameworks, due to the absence of the tube dynamics (18b) leading to simpler constraints.⁷ Compared to a nominal MPC, the additional complexity of the rigid tube MPC is mainly due to the geodesic computation in the initial condition (18e).

5 Conclusion

We have presented a robust adaptive MPC framework that uses a homothetic tube based on general CCMs and incorporates recursive model updates using set-membership estimation. We demonstrated the improved flexibility using a nonlinear example. Open-issues include the consideration of non-parametric model uncertainty and noisy output measurements.

Acknowledgements

This work has been supported by the Swiss National Science Foundation under NCCR Automation (grant agreement 51NF40 180545)

References

- [1] V. Adetola, D. DeHaan, and M. Guay. Adaptive model predictive control for constrained nonlinear systems. *Systems & Control Letters*, 58(5):320–326, 2009.
- [2] J.A.E. Andersson, J. Gillis, G. Horn, J.B. Rawlings, and M. Diehl. CasADi: a software framework for nonlinear optimization and optimal control. *Mathematical Programming Computation*, 11(1):1–36, 2019.
- [3] F. Bayer, M. Bürger, and F. Allgöwer. Discrete-time incremental ISS: A framework for robust NMPC. In *Proc. European Control Conf. (ECC)*, pages 2068–2073, 2013.
- [4] S. Chen, V. M. Preciado, M. Morari, and N. Matni. Robust Model Predictive Control with Polytopic Model Uncertainty through System Level Synthesis. *arXiv preprint arXiv:2203.11375*, 2023.
- [5] Luigi Chisci, J Anthony Rossiter, and Giovanni Zappa. Systems with persistent disturbances: predictive control with restricted constraints. *Automatica*, 37:1019–1028, 2001.
- [6] G. Chou, N. Ozay, and D. Berenson. Safe Output Feedback Motion Planning from Images via Learned Perception Modules and Contraction Theory. In *Proc. Algorithmic Foundations of Robotics XV*, pages 349–367. Springer, 2023.
- [7] M.H. Cohen, C. Belta, and R. Tron. Robust control barrier functions for nonlinear control systems with uncertainty: A duality-based approach. In *Proc. IEEE 61st Conference on Decision and Control (CDC)*, pages 174–179. IEEE, 2022.
- [8] A. Didier, A. Parsi, J. Coulson, and R.S Smith. Robust adaptive model predictive control of quadrotors. In *Proc. European Control Conference (ECC)*, pages 657–662. IEEE, 2021.

⁷ Among others, the tube dynamics (13d) require the expensive evaluation of $M(z) = W(z)^{-1}$. This inverse can also be avoided in the homothetic tube MPC by using the over-approximation $\bar{M} \succeq M(z)$ (cf. discussion Sec. 3.6).

- [9] F.A. Fontes. A general framework to design stabilizing nonlinear model predictive controllers. *Systems & Control Letters*, 42(2):127–143, 2001.
- [10] F.A. Fontes and L.T. Paiva. Guaranteed constraint satisfaction in continuous-time control problems. *IEEE Control Systems Letters*, 3(1):13–18, 2019.
- [11] L. Grüne and J. Pannek. *Nonlinear Model Predictive Control*. Springer, 2017.
- [12] M. Guay, V. Adetola, and D. DeHaan. *Robust and Adaptive Model Predictive Control of Nonlinear Systems*. Institution of Engineering and Technology, 2015.
- [13] L. Hewing, K.P. Wabersich, M. Menner, and M.N. Zeilinger. Learning-based model predictive control: Toward safe learning in control. *Annual Review of Control, Robotics, and Autonomous Systems*, 3:269–296, 2020.
- [14] B. Houska and M.E. Villanueva. Robust optimization for MPC. In *Handbook of model predictive control*, pages 413–443. Springer, 2019.
- [15] H.K. Khalil. *Nonlinear systems*. Patience Hall, 2002.
- [16] J. Köhler, E. Andina, R. Soloperto, M.A. Müller, and F. Allgöwer. Linear robust adaptive model predictive control: Computational complexity and conservatism. In *Proc. 58th IEEE Conference on Decision and Control (CDC)*, pages 1383–1388. IEEE, 2019. extended version on arXiv:1909.01813.
- [17] J. Köhler, P. Kötting, R. Soloperto, F. Allgöwer, and M.A. Müller. A robust adaptive model predictive control framework for nonlinear uncertain systems. *Int. J. Robust and Nonlinear Control*, 31(18):8725–8749, 2021.
- [18] J. Köhler, M. A. Müller, and F. Allgöwer. A nonlinear model predictive control framework using reference generic terminal ingredients. *IEEE Transactions on Automatic Control*, 65(8):3576–3583, 2019. extended version on arXiv:1909.12765.
- [19] J. Köhler, M.A. Müller, and F. Allgöwer. Robust output feedback model predictive control using online estimation bounds. *arXiv preprint arXiv:2105.03427*, 2021.
- [20] J. Köhler, R. Soloperto, M.A. Müller, and F. Allgöwer. A computationally efficient robust model predictive control framework for uncertain nonlinear systems. *IEEE Trans. Automat. Control*, 66(2):794–801, 2021. extended version online: arXiv:1910.12081.
- [21] B. Kouvaritakis and M. Cannon. *Model predictive control*. Springer, 2016.
- [22] A.P. Leeman, J. Köhler, A. Zanelli, S. Bennani, and M.N. Zeilinger. Robust Nonlinear Optimal Control via System Level Synthesis. *arXiv preprint arXiv:2301.04943*, 2023.
- [23] K. Leung and I.R. Manchester. Nonlinear stabilization via control contraction metrics: A pseudospectral approach for computing geodesics. In *Proc. 2017 American Control Conference (ACC)*, pages 1284–1289. IEEE, 2017.
- [24] D. Limon, A. Ferramosca, I. Alvarado, and T. Alamo. Nonlinear MPC for tracking piece-wise constant reference signals. *IEEE Trans. Automat. Control*, 63(11):3735–3750, 2018.
- [25] W. Lohmiller and J.J.E. Slotine. On contraction analysis for non-linear systems. *Automatica*, 34:683–696, 1998.
- [26] B.T. Lopez. *Adaptive robust model predictive control for nonlinear systems*. PhD thesis, Massachusetts Institute of Technology, 2019.
- [27] B.T. Lopez and J.J.E. Slotine. Universal adaptive control of nonlinear systems. *IEEE Control Systems Letters*, 6:1826–1830, 2021.
- [28] M. Lorenzen, M. Cannon, and F. Allgöwer. Robust MPC with recursive model update. *Automatica*, 103:461–471, 2019.
- [29] X. Lu and M. Cannon. Robust adaptive model predictive control with persistent excitation conditions. *Automatica*, 152:110959, 2023.
- [30] X. Lu, M. Cannon, and D. Koksál-Rivet. Robust adaptive model predictive control: Performance and parameter estimation. *Int. J. of Robust and Nonlinear Control*, 31(18):8703–8724, 2021.
- [31] S. Lucia. *Robust multi-stage nonlinear model predictive control*. Shaker Dortmund, 2015.
- [32] L. Magni and R. Scattolini. Model predictive control of continuous-time nonlinear systems with piecewise constant control. *IEEE Trans. Automat. Control*, 49(6):900–906, 2004.
- [33] I.R. Manchester and J.J.E. Slotine. Control contraction metrics: Convex and intrinsic criteria for nonlinear feedback design. *IEEE Trans. Automat. Control*, 62:3046–3053, 2017.
- [34] D.Q. Mayne, M.M. Seron, and S.V. Raković. Robust model predictive control of constrained linear systems with bounded disturbances. *Automatica*, 41:219–224, 2005.
- [35] A. Parsi, A. Iannelli, and R. Smith. Scalable tube model predictive control of uncertain linear systems using ellipsoidal sets. *International Journal of Robust and Nonlinear Control*, 2022.
- [36] A. Parsi, D. Liu, A. Iannelli, and R. Smith. Dual adaptive MPC using an exact set-membership reformulation. *arXiv preprint arXiv:2211.16300*, 2022.
- [37] G. Pin, D.M. Raimondo, L. Magni, and T. Parisini. Robust model predictive control of nonlinear systems with bounded and state-dependent uncertainties. *IEEE Trans. Automat. Control*, 54(7):1681–1687, 2009.
- [38] S.V. Raković, B. Kouvaritakis, R. Findeisen, and M. Cannon. Homothetic tube model predictive control. *Automatica*, 48(8):1631–1638, 2012.
- [39] S.V. Raković, L. Dai, and Y. Xia. Homothetic tube model predictive control for nonlinear systems. *IEEE Trans. Automat. Control*, 2022.
- [40] J.B. Rawlings, D.Q. Mayne, and M. Diehl. *Model Predictive Control: Theory, Computation, and Design*. Nob Hill Publishing, 2017. third printing.
- [41] J.D. Schiller, S. Muntwiler, J. Köhler, M.N. Zeilinger, and M.A. Müller. A Lyapunov function for robust stability of moving horizon estimation. *arXiv preprint arXiv:2202.12744*, 2022.
- [42] S. Singh, B. Landry, A. Majumdar, J.J. Slotine, and M. Pavone. Robust feedback motion planning via contraction theory. *Int. J. Robotics Research*, 2019. submitted.
- [43] S. Singh, A. Majumdar, J.J. Slotine, and M. Pavone. Robust online motion planning via contraction theory and convex optimization. In *Proc. Int. Conf. on Robotics and Automation (ICRA)*, pages 5883–5890, 2017.
- [44] M. Tanaskovic, L. Fagiano, R. Smith, and M. Morari. Adaptive receding horizon control for constrained MIMO systems. *Automatica*, 50(12):3019–3029, 2014.
- [45] M.E. Villanueva, R. Quirynen, M. Diehl, B. Chachuat, and B. Houska. Robust MPC via min–max differential inequalities. *Automatica*, 77:311–321, 2017.
- [46] K.P. Wabersich and M.N. Zeilinger. Nonlinear learning-based model predictive control supporting state and input dependent model uncertainty estimates. *Int. J. Robust Nonlinear Control*, 31(18):8897–8915, 2021.

- [47] A. Wächter and L.T. Biegler. On the implementation of an interior-point filter line-search algorithm for large-scale nonlinear programming. *Mathematical programming*, 106(1):25–57, 2006.
- [48] R. Wang, R. Tóth, and I.R. Manchester. Virtual control contraction metrics: Convex nonlinear feedback design via behavioral embedding. *arXiv preprint arXiv:2003.08513*, 2020.
- [49] S. Yu, C. Maier, H. Chen, and F. Allgöwer. Tube MPC scheme based on robust control invariant set with application to lipschitz nonlinear systems. *Systems & Control Letters*, 62:194–200, 2013.
- [50] A. Zanelli, J. Frey, F. Messerer, and M. Diehl. Zero-Order Robust Nonlinear Model Predictive Control with Ellipsoidal Uncertainty Sets. *IFAC-PapersOnLine*, 54(6):50–57, 2021. 7th IFAC Conference on Nonlinear Model Predictive Control NMPC 2021.
- [51] P. Zhao, A. Lakshmanan, K. Ackerman, A. Gahlawat, M. Pavone, and N. Hovakimyan. Tube-certified trajectory tracking for nonlinear systems with robust control contraction metrics. *IEEE Robotics and Automation Letters*, 7(2):5528–5535, 2022. extended version on arXiv:2109.04453.

A Appendix

In the following, we provide the proof of Proposition 2, which builds on established arguments from contraction theory [25, 33, 42], more specifically also [51, Thm. 1] and [41, App. A].

PROOF. Part I: Condition (8b) together with the definition of V_δ (9) implies Inequality (11a), cf., [41, Eq. (48)–(50)].

Part II: Recall that by assumption $(\gamma^*(s), \gamma^u(s)) \in \mathbb{Z}$ for all $s \in [0, 1]$, and $\left. \frac{d\gamma^u}{ds} \right|_s = K(\gamma^*(s))\gamma_s^*(s)$, cf., Equation (10). For any constant parameter $\bar{\theta} \in \Theta_0$, the differential dynamics along the geodesic are characterized by the Jacobian of the nonlinear system [51], i.e.,

$$\dot{\gamma}^*(s) = f_w(\gamma^*(s), \gamma^u(s), \bar{\theta} + s(\theta - \bar{\theta}), sd), \quad (\text{A.1})$$

$$\dot{\gamma}_s^*(s) = A_{cl}(\gamma^*(s), \gamma^u(s), \bar{\theta} + s(\theta - \bar{\theta}), sd)\gamma_s^*(s) + \gamma^w(s), \quad (\text{A.2})$$

$$\gamma^w(s) := G(\gamma^*(s), \gamma^u(s))(\theta - \bar{\theta}) + E(\gamma^*(s))d. \quad (\text{A.3})$$

Note that $\bar{\theta} + s(\theta - \bar{\theta}) \in \Theta_0$ and $sd \in \mathbb{D}$, $s \in [0, 1]$, since $0 \in \mathbb{D}$, and Θ_0, \mathbb{D} are convex. Let us define the following

abbreviations:

$$\begin{aligned} \hat{G}(s) &:= M(\gamma^*(s))^{\frac{1}{2}} G(\gamma^*(s), \gamma^u(s)), \\ \hat{E}(s) &:= M(\gamma^*(s))^{\frac{1}{2}} E(\gamma^*(s)), \\ G_{s,k}(z, v) &:= \frac{\partial \left(M^{\frac{1}{2}}[G]_{:,k} \right)}{\partial x} \Bigg|_{(z,v)} \\ &\quad + \frac{\partial \left(M^{\frac{1}{2}}[G]_{:,k} \right)}{\partial u} \Bigg|_{(z,v)} K(z), \\ E_{s,j}(z) &:= \frac{\partial \left(M^{\frac{1}{2}}[E]_{:,j} \right)}{\partial x} \Bigg|_z, \quad k \in \mathbb{I}_{[1,p]}, \quad j \in \mathbb{I}_{[1,q]}. \end{aligned}$$

Note that for any $\tilde{\theta} \in \mathbb{R}^p$ and any $d \in \mathbb{R}^q$, we have

$$\begin{aligned} \left. \frac{d\hat{G}}{ds} \right|_s \tilde{\theta} &= \sum_{k=1}^p [\tilde{\theta}]_k G_{s,k}(\gamma^*(s), \gamma^u(s)) \gamma_s^*(s), \\ \left. \frac{d\hat{E}}{ds} \right|_s d &= \sum_{j=1}^q [d]_j E_{s,j}(\gamma^*(s)) \gamma_s^*(s). \end{aligned}$$

Hence, for any $s \in [0, 1]$ it holds:

$$\begin{aligned} \|(\hat{G}(s) - \hat{G}(0))(\theta - \bar{\theta})\| &\leq \int_0^s \left\| \left. \frac{d\hat{G}}{ds} \right|_{\tilde{s}} (\theta - \bar{\theta}) \right\| d\tilde{s} \\ &= \int_0^s \left\| \sum_{k=1}^p G_{s,k}(\gamma^*(\tilde{s}), \gamma^u(\tilde{s})) [\theta - \bar{\theta}]_k \gamma_s^*(\tilde{s}) \right\| d\tilde{s} \\ &\leq \sum_{k=1}^p \|\theta - \bar{\theta}\|_k \int_0^s \left\| G_{s,k}(\gamma^*(\tilde{s}), \gamma^u(\tilde{s})) M(\gamma^*(\tilde{s}))^{-\frac{1}{2}} \right\| \\ &\quad \cdot \left\| M(\gamma^*(\tilde{s}))^{\frac{1}{2}} \gamma_s^*(\tilde{s}) \right\| d\tilde{s} \\ &\stackrel{(9)}{\leq} \sum_{k=1}^p L_{G,k} \|\theta - \bar{\theta}\|_k |V_\delta(x, z), \quad (\text{A.4}) \end{aligned}$$

with

$$L_{G,k} := \max_{(z,v) \in \mathbb{Z}} \left\| G_{s,k}(z, v) M(z)^{-\frac{1}{2}} \right\|, \quad k \in \mathbb{I}_{[1,p]}. \quad (\text{A.5})$$

Similarly, for any $s \in [0, 1]$, $d \in \mathbb{D}$, we get

$$\left\| (\hat{E}(s) - \hat{E}(0))d \right\| \leq L_{\mathbb{D}} |V_\delta(x, z), \quad (\text{A.6})$$

with

$$L_{\mathbb{D}} := \max_{z \in \mathbb{Z}_x, d \in \mathbb{D}} \left\| \sum_{j=1}^q E_{s,j}(z) M(z)^{-\frac{1}{2}} [d]_j \right\|. \quad (\text{A.7})$$

The above inequalities yield

$$\begin{aligned}
& \int_0^1 \gamma_s^*(s)^\top M(\gamma^*(s)) \gamma^w(s) ds \\
& \leq \int_0^1 \left\| \gamma_s^*(s)^\top \left(M(\gamma^*(s))^{\frac{1}{2}} \right)^\top \right\| \left(\left\| M(\gamma^*(0))^{\frac{1}{2}} \gamma^w(0) \right\| \right. \\
& \quad \left. + \left\| M(\gamma^*(s))^{\frac{1}{2}} \gamma^w(s) - M(\gamma^*(0))^{\frac{1}{2}} \gamma^w(0) \right\| \right) ds \\
& \stackrel{(9)}{\leq} V_\delta(x, z) \left(\|G(z, v)(\theta - \bar{\theta}) + E(z)d\|_{M(z)} \right. \\
& \quad \left. + \max_{s \in [0,1]} \left\| M(\gamma^*(s))^{\frac{1}{2}} \gamma^w(s) - M(\gamma^*(0))^{\frac{1}{2}} \gamma^w(0) \right\| \right) \\
& \stackrel{(A.4)}{\leq} \|G(z, v)(\theta - \bar{\theta}) + E(z)d\|_{M(z)} V_\delta(x, z) \\
& \stackrel{(A.6)}{\leq} \left(L_{\mathbb{D}} + \sum_{k=1}^p L_{G,k} |\theta - \bar{\theta}|_k \right) V_\delta(x, z)^2. \quad (A.8)
\end{aligned}$$

The Riemannian energy defined as

$\mathcal{E}(x, z) := \int_0^1 \gamma_s^*(s)^\top M(\gamma^*(s)) \dot{\gamma}_s^*(s) ds$ [33, 42, 51] satisfies

$$\begin{aligned}
\dot{\mathcal{E}}(x, z) &= \int_0^1 \gamma_s^*(s)^\top \dot{M}(\gamma^*(s)) \dot{\gamma}_s^*(s) \\
& \quad + \dot{\gamma}_s^*(s)^\top M(\gamma^*(s)) \dot{\gamma}_s^*(s) \\
& \quad + \gamma_s^*(s)^\top M(\gamma^*(s)) \dot{\gamma}_s^*(s) ds \\
& \stackrel{(A.1)(A.2)}{\leq} \int_0^1 -2\rho_c \gamma_s^*(s)^\top M(\gamma^*(s)) \dot{\gamma}_s^*(s) \\
& \quad + 2\gamma_s^*(s)^\top M(\gamma^*(s)) \gamma^w(s) ds \\
& \stackrel{(A.8)}{\leq} -2\rho_c \mathcal{E}(x, z) + 2V_\delta(x, z) \\
& \quad \cdot \left(\left(L_{\mathbb{D}} + \sum_{k=1}^p L_{G,k} |\theta - \bar{\theta}|_k \right) V_\delta(x, z) \right. \\
& \quad \left. + \|G(z, v)(\theta - \bar{\theta}) + E(z)d\|_{M(z)} \right). \quad (A.9)
\end{aligned}$$

Furthermore, since $\mathcal{E}(x, z) = V_\delta(x, z)^2$ (see [33, 43]), it holds that $\dot{\mathcal{E}}(x, z) = 2V_\delta(x, z)\dot{V}_\delta(x, z)$, and hence, Inequality (A.9) is equivalent to Condition (11b). \square